Large-Scale Shell-Model Analysis of the Neutrinoless $\beta\beta$ Decay of ^{48}Ca

Y. Iwata,[1,*] N. Shimizu,[1] T. Otsuka,[1,2,3,4] Y. Utsuno,[1,5] J. Menéndez,[2] M. Honma,[6] and T. Abe[2]
[1]Center for Nuclear Study, The University of Tokyo, 113-0033 Tokyo, Japan
[2]Department of Physics, The University of Tokyo, 113-0033 Tokyo, Japan
[3]National Superconducting Cyclotron Laboratory, Michigan State University, East Lansing, Michigan 48824, USA
[4]Instituut voor Kern- en Stralingsfysica, Katholieke Universiteit Leuven, B-3001 Leuven, Belgium
[5]Advanced Science Research Center, Japan Atomic Energy Agency, Tokai, 319-1195 Ibaraki, Japan
[6]Center for Mathematical Sciences, University of Aizu, 965-8580 Fukushima, Japan
(Received 13 November 2015; published 15 March 2016)

We present the nuclear matrix element for the neutrinoless double-beta decay of ^{48}Ca based on large-scale shell-model calculations including two harmonic oscillator shells (sd and pf shells). The excitation spectra of ^{48}Ca and ^{48}Ti, and the two-neutrino double-beta decay of ^{48}Ca are reproduced in good agreement to the experimental data. We find that the neutrinoless double-beta decay nuclear matrix element is enhanced by about 30% compared to pf-shell calculations. This reduces the decay lifetime by almost a factor of 2. The matrix-element increase is mostly due to pairing correlations associated with cross-shell sd-pf excitations. We also investigate possible implications for heavier neutrinoless double-beta decay candidates.

DOI: 10.1103/PhysRevLett.116.112502

The observation of neutrino oscillations established the massive nature of neutrinos almost two decades ago [1]. Despite great progress in neutrino physics in recent years [2], some fundamental properties are still unknown, like the Dirac or Majorana neutrino nature (whether they are their own antiparticle), or the absolute neutrino mass-scale and hierarchy. The first question would be answered with the detection of neutrinoless double-beta ($0\nu\beta\beta$) decay. In this lepton-number violating process, a nucleus decays into its isobar with two less neutrons and two more protons, emitting two electrons and no (anti)neutrinos. Several international collaborations are running experiments to measure this process [3–6] or plan to do it in the near future [7–12], and have set impressive lower limits for the $0\nu\beta\beta$ decay lifetimes, $T^{0\nu}_{1/2} > 10^{25}$ yr, for the most favorable cases.

In addition, $0\nu\beta\beta$ decay can determine the absolute neutrino masses and hierarchy if the nuclear matrix element (NME) of the transition $M^{0\nu}$ is accurately known. The lifetime of the decay reads [13]

$$[T^{0\nu}_{1/2}(0^+_i \to 0^+_f)]^{-1} = G^{0\nu}|M^{0\nu}|^2 \left(\frac{\langle m_{\beta\beta}\rangle}{m_e}\right)^2, \quad (1)$$

with 0^+_i (0^+_f) the initial (final) state, $G^{0\nu}$ a well-known phase-space factor [14], and $\langle m_{\beta\beta}\rangle$ a combination of the absolute neutrino masses and the neutrino mixing matrix (the electron mass m_e is introduced by convention).

Calculated NME values, however, differ by factors of 2 or 3 depending on the theoretical nuclear structure approaches used. This uncertainty severely limits the potential capability to determine the absolute neutrino masses with $0\nu\beta\beta$ decay. Among the NME calculations, shell-model results [15–17] are typically at the lower end, and it has been argued that this may be due to the relatively small configuration space that can be accessed by present shell-model codes [18]. On the other hand, within the configuration space where the calculation is performed, the shell model can include various additional correlations compared to other approaches that yield larger NME values [19–21], like the quasiparticle random-phase approximation (QRPA) [22–24], the interacting boson model (IBM) [25], the energy density functional (EDF) [26,27], or the generator coordinate method (GCM) [28].

The doubly magic ^{48}Ca is the lightest isotope considered in $\beta\beta$ decay searches, including the CARVEL [29], CANDLES [7,30,31], and NEMO-III [32] experiments. Its $\beta\beta$ decay into ^{48}Ti is ideally suited for shell-model calculations, which are very successful in this mass region for a wide variety of observables [33]. In fact, the two-neutrino double-beta ($2\nu\beta\beta$) decay lifetime was predicted by a shell-model calculation [34] in very good agreement with the subsequent experimental detection [35].

In this Letter, we present an improved calculation of the $0\nu\beta\beta$ decay NME for ^{48}Ca based on the large-scale shell model in two harmonic oscillator shells (sd and pf shells). This significantly expands previous shell-model studies performed in the pf shell [15–17,19], increasing the number of single-particle orbitals from four to seven. We use the M-scheme shell-model code KSHELL [36], and allow up to $2\hbar\omega$ sd-pf cross-shell excitations. The dimension of the largest calculation (^{48}Ti) is 2.0×10^9.

We use the shell-model SDPFMU effective interaction [37], which describes well the shell evolution and the spectroscopy of neutron-rich nuclei in the upper sd shell. The pf-shell part of this interaction is based on the GXPF1B interaction, which accounts very successfully for the spectroscopy of pf-shell nuclei [38,39]. While the

SDPFMU interaction works reasonably well, a slightly revised one, SDPFMU-DB, is introduced by reducing the shell gap of ^{40}Ca to 5.8 MeV so as to reproduce the observed 0_2^+ level of ^{48}Ca. The two-proton transfer reaction experiment [40] shows a large cross section to the 0_2^+ state of ^{48}Ca, suggesting sizable proton excitations from the sd shell. The 0_2^+ state obtained with the SDPFMU-DB interaction shows 1.64 protons in the pf shell consistently with this property, whereas the SDPFMU result finds only 0.22. The new SDPFMU-DB interaction thus gives an improved description compared to SDPFMU.

Figure 1 shows the excitation spectra of ^{48}Ca and ^{48}Ti obtained with SDPFMU-DB, which are in good agreement with the experimental data. The SDPFMU spectra are generally of similar quality, with the 0_2^+ level of ^{48}Ca too high by 200 keV. In contrast, a pf-shell calculation with GXPF1B gives the 0_2^+ level in ^{48}Ca 1.3 MeV higher than the experimental one. For the 0_2^+ state in ^{48}Ti, the $sdpf$-shell calculation with SDPFMU-DB gives 1.0 MeV higher excitation energy than experiment, probably due to missing $4\hbar\omega$ excitations. The $2\hbar\omega$ components in the ground states of ^{48}Ca and ^{48}Ti are 22% and 33% for SDPFMU-DB (14% and 20% for SDPFMU). Such sizable $2\hbar\omega$ excitations suggest that these interactions in the $sdpf$-configuration space capture sufficiently well cross-shell sd-pf excitations.

First, we study the $2\nu\beta\beta$ decay of ^{48}Ca. We calculate the Gamow-Teller β^+ and β^- strengths [42], and compare them to experiments for the energy range up to 5 MeV [43,44], so that we can extract the appropriate quenching factor q of the $\sigma\tau$ operator for each calculation. We find $q = 0.71$ for both $sdpf$ interactions, and $q = 0.74$ for the pf-shell interaction, in accordance with previous pf-shell studies [33]. The similar quenching factor shows that it does not depend on missing sd-pf correlations. Then we calculate $2\nu\beta\beta$ decay matrix elements by summing contributions from 100 virtual 1^+ intermediate states in ^{48}Sc, and obtain $M^{2\nu} = 0.051$ (0.045) MeV^{-1} with the SDPFMU-DB (SDPFMU) interaction, in good agreement with the experimental value, $M^{2\nu} = 0.046 \pm 0.004$ MeV^{-1} [45]. In the pf-shell calculation with GXPF1B the result is very similar, $M^{2\nu} = 0.052$ MeV^{-1}, reflecting low sensitivity to the size of the shell-model configuration space in $2\nu\beta\beta$ decay. This is in contrast to the high sensitivity observed in Ref. [46]. The difference arises because in the present calculations all spin-orbit partners are always included.

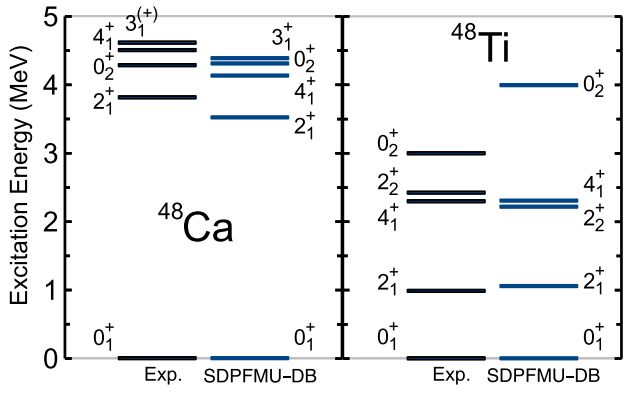

FIG. 1. Excitation spectra of ^{48}Ca and ^{48}Ti. The lowest five positive-parity states [41] are compared to $sdpf$ calculations with the SDPFMU-DB interaction.

We then calculate the ^{48}Ca $0\nu\beta\beta$ decay NME in the $sdpf$ space including up to $2\hbar\omega$ configurations. It is given in the closure approximation as [13]

$$M^{0\nu} = \langle 0_f^+ | \hat{O}^{0\nu} | 0_i^+ \rangle = M_{\rm GT}^{0\nu} - \frac{g_V^2}{g_A^2} M_{\rm F}^{0\nu} + M_{\rm T}^{0\nu}, \quad (2)$$

with Gamow-Teller ($M_{\rm GT}^{0\nu}$), Fermi ($M_{\rm F}^{0\nu}$), and tensor ($M_{\rm T}^{0\nu}$) terms classified according to the spin structure of the operator. The vector and axial coupling constants are taken to be $g_V = 1$ and $g_A = 1.27$, respectively. We set the closure parameter to $\langle E \rangle = 0.5$ MeV, found appropriate in the pf-shell calculation of Ref. [17]. We consider the inclusion of Argonne- and CD-Bonn-type short range correlations [47]. Two-body current contributions to the transition operator [48] are not included. The possible quenching of the $\sigma\tau$ operator in $0\nu\beta\beta$ decay is the matter of discussion [18], because compared to $2\nu\beta\beta$ decay the momentum transfer is larger, and the virtual intermediate states of the transition include additional multipolarities. Therefore, similarly to most previous calculations, we do not quench the $\sigma\tau$ operator for $0\nu\beta\beta$ decay. A detailed discussion on the $0\nu\beta\beta$ decay operator $\hat{O}^{0\nu}$ can be found in Ref. [16].

The calculated values of the NME are shown in Table I. The Gamow-Teller and Fermi parts, $M_{\rm GT}^{0\nu}$ and $M_{\rm F}^{0\nu}$, are enhanced in the $2\hbar\omega$ calculations by about (20–40)% compared to the pf-shell calculations. The largest values are given by the SDPFMU-DB interaction, which allows a stronger mixing of $2\hbar\omega$ configurations in the mother and daughter nuclei. The tensor contribution $M_{\rm T}^{0\nu}$ is almost unaffected by enlarging the configuration space. The 10% difference between the NME values obtained with the two $sdpf$ shell-model interactions is similar to the uncertainty obtained with different pf-shell interactions [16]. The sensitivity to short-range correlations is about 10%. Using the closure parameter $\langle E \rangle = 7.72$ MeV of Refs. [15,16], the NME value is reduced by around 5%.

Additional correlations beyond the sd-pf space are potentially relevant for the ^{48}Ca NME. To evaluate its effect, we have performed a $2\hbar\omega$ calculation including the pf and sdg shells, using the interaction from Ref. [49], which describes well negative parity states in neutron-rich calcium isotopes (sensitive to pf-sdg excitations). We find a small 5% change in the NME compared to the pf-shell result, consistent with the small cross-shell pf-sdg excitations (about 2%) in ^{48}Ca and ^{48}Ti. This suggests that the sd-pf space captures the most relevant correlations beyond the pf shell for the ^{48}Ca NME.

TABLE I. NME value for the ^{48}Ca $0\nu\beta\beta$ decay. The pf-shell calculation with GXPF1B is compared to the $sdpf$ $2\hbar\omega$ results obtained with the SDPFMU-DB and SDPFMU interactions. Total values ($M^{0\nu}$) are shown together with Gamow-Teller ($M^{0\nu}_{\rm GT}$), Fermi ($M^{0\nu}_{\rm F}$), and tensor ($M^{0\nu}_{\rm T}$) parts. Argonne- and CD-Bonn-type short-range correlations (SRC) are considered.

	GXPF1B				SDPFMU-DB				SDPFMU			
SRC	$M^{0\nu}_{\rm GT}$	$M^{0\nu}_{\rm F}$	$M^{0\nu}_{\rm T}$	$M^{0\nu}$	$M^{0\nu}_{\rm GT}$	$M^{0\nu}_{\rm F}$	$M^{0\nu}_{\rm T}$	$M^{0\nu}$	$M^{0\nu}_{\rm GT}$	$M^{0\nu}_{\rm F}$	$M^{0\nu}_{\rm T}$	$M^{0\nu}$
None	0.776	−0.216	−0.077	0.833	0.997	−0.304	−0.067	1.118	0.894	−0.291	−0.068	1.007
CD-Bonn	0.809	−0.233	−0.074	0.880	1.045	−0.327	−0.065	1.183	0.939	−0.313	−0.065	1.068
Argonne	0.743	−0.213	−0.075	0.801	0.953	−0.300	−0.065	1.073	0.852	−0.288	−0.068	0.963

Figure 2 compares different NME calculations for ^{48}Ca. The total NME value in the $sdpf$ configuration space, $M^{0\nu} = 0.96 - 1.18$, is about 30% larger than the pf-shell GXPF1B result or other shell-model pf-shell values $M^{0\nu} = 0.78 - 0.92$ [15–17]. This enhancement has important consequences for ^{48}Ca $0\nu\beta\beta$ decay experiments, as the decay lifetime is almost halved. The present NME value is 15% smaller than the result obtained by a pf-shell calculation including perturbatively the effect of the orbitals outside the pf configuration space, $M^{0\nu} = 1.30$ [50]. In contrast, Fig. 2 shows that the present NME value is considerably smaller than IBM [25], nonrelativistic [26] or relativistic [27] EDF values, and significantly larger than the QRPA result [22].

In the following, we analyze the NME to understand the mechanisms responsible for the enhancement found in the $2\hbar\omega$ calculations, and explore possible implications for heavier $0\nu\beta\beta$ decay candidates. The operator for the NME can be decomposed in terms of the angular momentum and parity J^π, to which the two-decaying neutrons are coupled [18]:

$$M^{0\nu} = \sum_J \langle 0^+_f | \sum_{i\le j,k\le l} M^J_{ij,kl} [(\hat{a}^\dagger_i \hat{a}^\dagger_j)^J (\hat{a}_k \hat{a}_l)^J]^0 | 0^+_i \rangle, \quad (3)$$

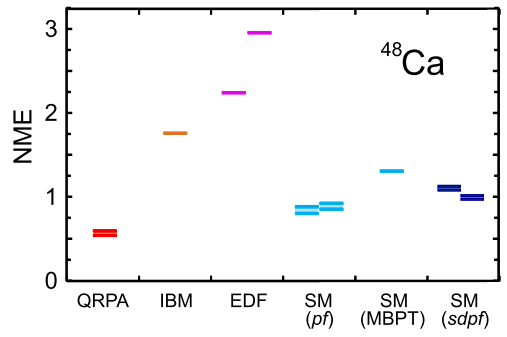

FIG. 2. Comparison of NME values for the ^{48}Ca $0\nu\beta\beta$ decay. The present shell-model results in the $sdpf$ space (SM $sdpf$: left SDPFMU-DB, right SDPFMU) are compared to pf-shell results (SM pf: left [17], right [15]), pf-shell result plus a perturbative calculation of the effect of orbitals outside the pf shell (SM MBPT) [50], QRPA [22], IBM [25], and EDF (left: nonrelativistic [26], right: relativistic [27]) calculations. The range between double horizontal bars covers results including a different type of short-range correlations (Argonne, CD-Bonn, UCOM [51]) and without them.

where i, j, k, l label single-particle orbitals. This decomposition is shown in Fig. 3 for $0\hbar\omega$ (pf) and $2\hbar\omega$ ($sdpf$) calculations. The leading contribution to $0\nu\beta\beta$ decay comes from 0^+-coupled pairs, while other J^π combinations suppress the NME. Figure 3 shows that the main difference between the $0\hbar\omega$ and $2\hbar\omega$ results is a 20% increase in the contributions of 0^+ pairs. In addition, only the $2\hbar\omega$ calculation allows for negative-parity pairs, but their contribution is small. As also suggested in Ref. [52], these findings indicate that the NME is enhanced by the pairing correlations, which induce 0^+-pair excitations, introduced by the additional sd-shell orbitals.

We further decompose the NME in terms of the orbitals (sd or pf shell) occupied by the two ^{48}Ca neutrons and two ^{48}Ti protons involved in the decay:

$$M^{0\nu} = \mathcal{M}^{0\nu}_1 + \mathcal{M}^{0\nu}_2 + \mathcal{M}^{0\nu}_3 + \mathcal{M}^{0\nu}_4 + \mathcal{M}^{0\nu}_5, \quad (4)$$

with the $\mathcal{M}^{0\nu}$ components, sketched in Fig. 4, defined as

$$\begin{aligned}
\mathcal{M}^{0\nu}_1 &= \langle 0^+_f | \hat{O}^{0\nu}(p_{pf}p_{pf}; n_{pf}n_{pf}) | 0^+_i \rangle, \\
\mathcal{M}^{0\nu}_2 &= \langle 0^+_f | \hat{O}^{0\nu}(p_{pf}p_{pf}; n_{sd}n_{sd}) | 0^+_i \rangle, \\
\mathcal{M}^{0\nu}_3 &= \langle 0^+_f | \hat{O}^{0\nu}(p_{sd}p_{sd}; n_{pf}n_{pf}) | 0^+_i \rangle, \\
\mathcal{M}^{0\nu}_4 &= \langle 0^+_f | \hat{O}^{0\nu}(p_{sd}p_{sd}; n_{sd}n_{sd}) | 0^+_i \rangle, \\
\mathcal{M}^{0\nu}_5 &= \langle 0^+_f | \hat{O}^{0\nu}(p_{sd}p_{pf}; n_{sd}n_{pf}) | 0^+_i \rangle, \quad (5)
\end{aligned}$$

where n_i (p_i) stands for neutrons (protons) in the i shell of ^{48}Ca (^{48}Ti). Table II shows the different components in Eq. (4) for the SDPFMU-DB $2\hbar\omega$ calculation, as well as

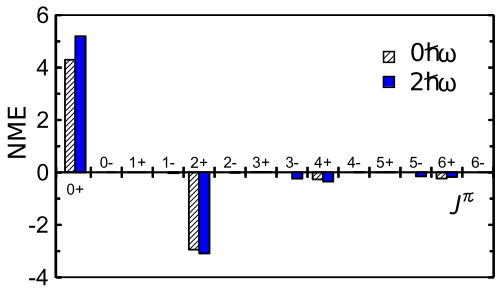

FIG. 3. NME decomposition in terms of the angular momentum and parity J^π of the pair of decaying neutrons, Eq. (3). $0\hbar\omega$ (GXPF1B) and $2\hbar\omega$ (SDPFMU-DB) results are compared, without short-range correlations.

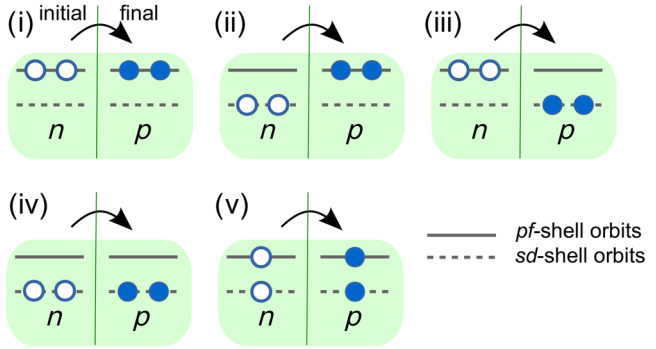

FIG. 4. Diagrams associated with the NME decomposition in Eq. (4), classified in terms of the sd- or pf-shell orbitals occupied by the decaying neutrons (open circles) and created protons (filled circles). Initial (final) stands for ^{48}Ca (^{48}Ti). Diagrams (i)–(v) correspond to $\mathcal{M}_1^{0\nu} - \mathcal{M}_5^{0\nu}$, respectively.

their decomposition in terms of the J^π of the decaying neutron pair [cf. Eq. (3)]. $\mathcal{M}_1^{0\nu}$, the only term allowed in the $0\hbar\omega$ calculation, is very similar in the pf and $sdpf$ spaces. On the contrary, $\mathcal{M}_2^{0\nu}$, $\mathcal{M}_3^{0\nu}$, and $\mathcal{M}_4^{0\nu}$ require $2\hbar\omega$ excitations in the mother and/or daughter nuclei (see Fig. 4). In fact, these terms are responsible for the enhancement of the NME in the $sdpf$ configuration space. Table II shows that, for $\mathcal{M}_2^{0\nu}$, $\mathcal{M}_3^{0\nu}$, and $\mathcal{M}_4^{0\nu}$, the contribution of 0^+ pairs is dominant, about 3 times larger in magnitude than the other J^π pairs. This is in contrast to $\mathcal{M}_1^{0\nu}$, or pf-shell calculations, where the contribution of the 0^+ terms is 30% larger than the other J^π pairs. These results confirm that the pairing correlations inducing neutron and proton cross-shell sd-pf excitations are responsible for the enhancement of the NME.

The remaining term $\mathcal{M}_5^{0\nu}$ requires the two nucleons being in different orbitals [see Fig. 4, diagram (v)]. These two neutrons cannot be coupled to $J^\pi = 0^+$, and are not involved in the 0^+ pair contributions. They instead produce strong cancellations, as shown in Table II, consistently with the $J^\pi \neq 0^+$ contributions in Fig. 3.

The above discussion suggests that the enlargement of the model space produces two competing mechanisms to be considered in all $0\nu\beta\beta$ decays. On the one hand, additional pairing correlations in the mother and daughter nuclei, enhanced by two-particle–two-hole ($2p$-$2h$) excitations with respect to the original configuration space, increase the NME values, as seen in $\mathcal{M}_1^{0\nu} - \mathcal{M}_4^{0\nu}$ for the ^{48}Ca decay. On the other hand, excitations in the initial and final nuclei outside the original space can increase $J^\pi \neq 0^+$ contributions as well. Assuming that these follow the same trends as in Fig. 3, this second mechanism will reduce the NME value, as seen in $\mathcal{M}_5^{0\nu}$ for ^{48}Ca. Important contributions come from one-particle–one-hole ($1p$-$1h$) excitations. For the ^{48}Ca decay, however, $1p$-$1h$ excitations always change parity and do not contribute to 0^+ ground states, and this mechanism remains rather modest.

TABLE II. NME decomposition of Eq. (4), for a $sdpf$ $2\hbar\omega$ SDPFMU-DB calculation without short-range correlations. The total value is shown along with the contributions of $J^\pi = 0^+$ and all remaining pairs.

	$\mathcal{M}_1^{0\nu}$	$\mathcal{M}_2^{0\nu}$	$\mathcal{M}_3^{0\nu}$	$\mathcal{M}_4^{0\nu}$	$\mathcal{M}_5^{0\nu}$
Total	0.915	0.168	0.269	0.220	−0.454
$J^\pi = 0^+$	4.193	0.364	0.379	0.255	0.000
$J^\pi = 0^-, J > 0$	−3.278	−0.196	−0.109	−0.035	−0.454

For heavier nuclei, these two competing effects need to be calculated in detail. While pairing correlations are most important for $0\nu\beta\beta$ decay, $1p$-$1h$ type excitations have smaller unperturbed energy difference than $2p$-$2h$ excitations, and can be sizable. The balance between the two mechanisms will determine the NME. For example, Ref. [46] found a 35% smaller NME value for ^{136}Xe when including up to $1p$-$1h$ excitations into the missing spin-orbit partners in the original shell-model configuration space. In contrast, Ref. [53] found a 20% increase in the ^{82}Se and ^{136}Xe NME values when considering $2p$-$2h$ excitations. A related competition between opposite-sign contributions was very recently suggested in Ref. [54] for ^{76}Ge.

Finally, we estimate the NME beyond $2\hbar\omega$ sd-pf excitations. An exact diagonalization in the full $sdpf$ configuration space is not feasible with present computing capabilities. However, this space can be handled in a seniority-zero approximation, that is, in a basis with all nucleons coupled in like-particle $J^\pi = 0^+$ pairs. In a given configuration space the NME is maximum in this limit, as higher seniority components only reduce its value [19]. A full $sdpf$ seniority-zero calculation with SDPFMU-DB, performed with the J-coupled code NATHAN [33], shows that components beyond $2\hbar\omega$ excitations are negligible (less than 0.5%) in both ^{48}Ca and ^{48}Ti. That is, $N\hbar\omega$ excitations ($N > 2$) only contribute to high seniorities; thus, they can only reduce the NME. This implies that the $sdpf$ pairing correlations enhancing $0\nu\beta\beta$ decay are completely captured by the $2\hbar\omega$ configurations included in the present calculations, and consequently the results obtained in this Letter provide an upper bound for the NME value in the full $sdpf$ configuration space.

In summary, we have carried out large-scale shell-model calculations of ^{48}Ca and ^{48}Ti, for the first time including up to $2\hbar\omega$ excitations in the $sdpf$ space. The excitation spectra of ^{48}Ca and ^{48}Ti, and the $2\nu\beta\beta$ decay of ^{48}Ca are reproduced in good agreement to experiment. We find different sensitivities to the configuration-space size in $\beta\beta$ decays; while the $2\nu\beta\beta$ decay NME is similar in the pf and $sdpf$ shells, the $0\nu\beta\beta$ decay NME increases by about 30% to $M^{0\nu} \approx 1.1$. The NME enhancement, which almost halves the associated decay life time, is due to cross-shell sd-pf pairing correlations. A seniority analysis shows that pairing effects in the $sdpf$ space are completely captured by the

$2\hbar\omega$ calculations, so that the present result suggests an upper value for the NME in the full $sdpf$ space.

Correlations outside the sd-pf space have been evaluated to be small. Beyond present shell-model capabilities, they can be estimated with many-body perturbation theory (MBPT) [50] or GCM [21,28] techniques, complementing the present result. Further efforts are needed to set a more definitive value for the ^{48}Ca $0\nu\beta\beta$ decay NME, for instance, by further enlarging the model space, improving the closure approximation, introducing two-body currents and/or a renormalization of the operator for the model space. Future plans include calculating NMEs for heavier $0\nu\beta\beta$ decay candidates in extended shell-model configuration spaces. For these isotopes, competition between $1p$-$1h$ and pairing like $2p$-$2h$ excitations in the present context will be of much interest, and their subtle balance should be evaluated precisely to obtain reliable NMEs.

This work was supported in part by Grants-in-Aid for Scientific Research (No. 23244049, No. 25870168, No. 26·04323, No. 15H01029). It was supported also in part by HPCI Strategic Program (hp150224) and CNS-RIKEN joint project for large-scale nuclear structure calculations. J. M. was supported by an International Research Fellowship from JSPS. Numerical calculations were carried out at FX10 (The University of Tokyo), K computer (RIKEN AICS), and COMA (University of Tsukuba).

*iwata@cns.s.u-tokyo.ac.jp

[1] Y. Fukuda *et al.*, Phys. Rev. Lett. **81**, 1562 (1998).
[2] M. C. Gonzalez-Garcia, M. Maltoni, and T. Schwetz, J. High Energy Phys. 11 (2014) 052.
[3] J. B. Albert *et al.* (EXO Collaboration), Nature (London) **510**, 229 (2014).
[4] A. Gando *et al.* (KamLAND-Zen Collaboration), Phys. Rev. Lett. **110**, 062502 (2013).
[5] M. Agostini *et al.* (GERDA Collaboration), Phys. Rev. Lett. **111**, 122503 (2013).
[6] K. Alfonso *et al.* (CUORE Collaboration), Phys. Rev. Lett. **115**, 102502 (2015).
[7] S. Umehara *et al.*, EPJ Web Conf. **66**, 08008 (2014).
[8] N. Abgrall *et al.* (MAJORANA Collaboration), Adv. High Energy Phys. **2014**, 365432 (2014).
[9] J. J. Gómez Cadenas *et al.* (NEXT Collaboration), Adv. High Energy Phys. **2014**, 907067 (2014).
[10] N. Bongrand *et al.* (SuperNEMO Collaboration), Phys. Procedia **61**, 211 (2015).
[11] B. Wonsak *et al.* (COBRA Collaboration), Phys. Procedia **61**, 295 (2015).
[12] V. Lozza *et al.* (SNO+ Collaboration), EPJ Web Conf. **65**, 01003 (2014).
[13] F. T. Avignone III, S. R. Elliott, and J. Engel, Rev. Mod. Phys. **80**, 481 (2008).
[14] J. Kotila and F. Iachello, Phys. Rev. C **85**, 034316 (2012).
[15] J. Menéndez, A. Poves, E. Caurier, and F. Nowacki, Nucl. Phys. **A818**, 139 (2009).
[16] M. Horoi and S. Stoica, Phys. Rev. C **81**, 024321 (2010).
[17] R. A. Sen'kov and M. Horoi, Phys. Rev. C **88**, 064312 (2013).
[18] P. Vogel, J. Phys. G **39**, 124002 (2012).
[19] E. Caurier, J. Menéndez, F. Nowacki, and A. Poves, Phys. Rev. Lett. **100**, 052503 (2008).
[20] J. Menéndez, T. R. Rodríguez, G. Martínez-Pinedo, and A. Poves, Phys. Rev. C **90**, 024311 (2014).
[21] J. Menéndez, N. Hinohara, J. Engel, G. Martínez-Pinedo, and T. R. Rodríguez, Phys. Rev. C **93**, 014305 (2016).
[22] F. Šimkovic, V. Rodin, A. Faessler, and P. Vogel, Phys. Rev. C **87**, 045501 (2013).
[23] J. Hyvärinen and J. Suhonen, Phys. Rev. C **91**, 054308 (2015).
[24] J. Terasaki, Phys. Rev. C **91**, 034318 (2015).
[25] J. Barea, J. Kotila, and F. Iachello, Phys. Rev. C **91**, 034304 (2015).
[26] N. L. Vaquero, T. R. Rodríguez, and J. L. Egido, Phys. Rev. Lett. **111**, 142501 (2013).
[27] J. M. Yao, L. S. Song, K. Hagino, P. Ring, and J. Meng, Phys. Rev. C **91**, 024316 (2015).
[28] N Hinohara and J. Engel, Phys. Rev. C **90**, 031301(R) (2014).
[29] Yu. G. Zdesenko, F. T. Avignone, V. B. Brudanin, F. A. Danevich, V. V. Kobychev, B. N. Kropivyansky, S. S. Nagorny, V. I. Tretyak, and Ts. Vylov, Astropart. Phys. **23**, 249 (2005).
[30] S. Umehara *et al.*, Phys. Rev. C **78**, 058501 (2008).
[31] T. Kishimoto, K. Matsuoka, T. Fukumoto, and S. Umehara, Prog. Theor. Exp. Phys. **2015**, 33D03 (2015).
[32] A. S. Barabash and V. B. Brudanin (NEMO Collaboration), Phys. At. Nucl. **74**, 312 (2011).
[33] E. Caurier, G. Martínez-Pinedo, F. Nowacki, A. Poves, and A. P. Zuker, Rev. Mod. Phys. **77**, 427 (2005).
[34] E. Caurier, A. Poves, and A. P. Zuker, Phys. Lett. B **252**, 13 (1990).
[35] A. Balysh, A. De Silva, V. I. Lebedev, K. Lou, M. K. Moe, M. A. Nelson, A. Piepke, A. Pronskiy, M. A. Vient, and P. Vogel, Phys. Rev. Lett. **77**, 5186 (1996).
[36] N. Shimizu, arXiv:1310.5431.
[37] Y. Utsuno, T. Otsuka, B. A. Brown, M. Honma, T. Mizusaki, and N. Shimizu, Phys. Rev. C **86**, 051301(R) (2012).
[38] M. Honma *et al.*, RIKEN Accelerator Progress Report **41**, 32 (2008).
[39] M. Honma, T. Otsuka, B. A. Brown, and T. Mizusaki, Eur. Phys. J. A **25**, Suppl. 1, 499 (2005).
[40] F. Videbaek, O. Hansen, M. J. Levine, C. Ellegaard, S. D. Hoath, and J. M. Nelson, Nucl. Phys. **A451**, 131 (1986).
[41] NuDat 2.6, http://www.nndc.bnl.gov/nudat2/.
[42] Y. Iwata, N. Shimizu, Y. Utsuno, M. Honma, T. Abe, and T. Otsuka, JPS Conf. Proc. **6**, 030057 (2015).
[43] E. W. Grewe *et al.*, Phys. Rev. C **76**, 054307 (2007).
[44] K. Yako *et al.*, Phys. Rev. Lett. **103**, 012503 (2009).
[45] A. S. Barabash, Nucl. Phys. **A935**, 52 (2015).
[46] M. Horoi and B. A. Brown, Phys. Rev. Lett. **110**, 222502 (2013).
[47] F. Šimkovic, A. Faessler, H. Muther, V. Rodin, and M. Stauf, Phys. Rev. C **79**, 055501 (2009).

[48] J. Menéndez, D. Gazit, and A. Schwenk, Phys. Rev. Lett. **107**, 062501 (2011).
[49] Y. Utsuno, T. Otsuka, B. A. Brown, M. Honma, T. Mizusaki, and N. Shimizu, Prog. Theor. Phys. Suppl. **196**, 304 (2012).
[50] A. A. Kwiatkowski *et al.*, Phys. Rev. C **89**, 045502 (2014).
[51] R. Roth, H. Hergert, P. Papakonstantinou, T. Neff, and H. Feldmeier, Phys. Rev. C **72**, 034002 (2005).
[52] B. A. Brown, M. Horoi, and R. A. Sen'kov, Phys. Rev. Lett. **113**, 262501 (2014).
[53] E. Caurier, F. Nowacki, and A. Poves, Eur. Phys. J. A **36**, 195 (2008).
[54] B. A. Brown, D. L. Fang, and M. Horoi, Phys. Rev. C **92**, 041301(R) (2015).